

33 limitations is the process of singlet fission (SF). This process can double photocur-
34 rent and PCE beyond the theoretical Shockley Queisser limit for single-junction
35 solar cells by splitting a high-energy singlet exciton into two lower-energy triplet
36 excitons.^{9–13} SF has been a rich area of study in materials chemistry, photo-physics,
37 and device engineering since its initial observation in anthracene crystals in the
38 1960s.^{14–16} Research has shown that SF efficiency is closely dependent on the
39 molecular electronic structure and intermolecular packing, as well as the energy
40 alignment between the singlet and triplet states.^{17–19} A chromophore that under-
41 goes SF should have a singlet energy (E_{S1}) slightly greater than $2E_{T1}$, in addition
42 to good orbital overlap and crystal shape to allow for fast triplet fission and
43 movement.^{20–24} Recent advances in computational quantum chemistry, particularly
44 the application of density functional theory (DFT), have enabled the theoretical
45 prediction, screening, and optimization of novel singlet fission (SF)–active mater-
46 ials prior to their computational synthesis. DFT methods provide reasonable
47 accuracy along with efficiency and thus enable the rational design of π -conjugated
48 organic molecules to the d and SF chromophores for incorporation into OSCs.^{25–26}
49 Of particular significance is the fact that now, computational descriptors such as
50 frontier orbital gaps, singlet–triplet energy splitting (ΔE_{ST}), and even intersystem
51 crossing rates are routinely calculated and benchmarked against designed data to
52 expedite discovery.²⁷ In the past decade alone, there has been a surge in theoretical
53 and empirical research focused on the development of acene and heteroacene SF
54 materials, diketopyrrolopyrroles and perylenediimides, as well as other π -extended
55 scaffolds.²⁸ Rational core modification through heteroatom doping, functional group
56 engineering, and controlled molecular packing has provided diverse materials with
57 greater photostability, increased OSC compatibility, faster SF rates, and even
58 enhanced OSC compatibility.²⁹ Direct measurement and utilization of triplet
59 yields made possible by ultrafast spectroscopic techniques and advanced device
60 architectures have confirmed computational estimates and further enabled iterative
61 molecular design. During the past three years, studies have emphasized the increas-
62 ing synergy between high-throughput DFT screening and machine learning, which
63 has enabled the accelerated prediction of SF chromophores with unprecedented
64 scope and precision.³⁰ Significant advancements in donor–acceptor copolymers,
65 non-fullerene acceptors, and hybrid organic–inorganic interfaces utilizing SF to
66 enhance OSC efficiencies beyond 20% have been published in Elsevier-indexed
67 journals.³¹ These advances have been aided by multiscale modeling approaches,
68 including TD-DFT, GW-BSE methods and excited-state dynamics simulations,
69 which provide atomic-level insights into the structure-property relationships
70 governing SF and triplet harvesting. Despite these advancements, critical issues
71 remain. Many proposed SF materials are hindered by challenges including
72 synthetic inaccessibility, instability, or poor integration into device architectures.
73 The chromophore energy levels, solid-state morphology, and interface design still

102 energy splitting (ΔE_{ST}). These properties are critical determinants for assessing the likelihood
 103 that a molecule can undergo efficient singlet fission. All parameters calculated are presented in
 104 Table II.

105 TABLE I. Novel chromophores and their key structural groups

Code	Compound name	Key structural group(s)
N1	naphtho[2,3- <i>b</i> :6,7- <i>c'</i>]bis(borinine)	boron
N2	2 <i>H</i> -selenopheno[2,3- <i>b</i>]indole-3,6-dione	selenophene, dione
N3	thieno[2',3':4,5]pyrido[1,2- <i>b</i>]indazole	aza, thiophene
N4	4,7-bis((triisopropylsilyl)ethynyl)-3 <i>aH</i> -thieno[2,3- <i>b</i>]indole	TIPS, thienoindole
N5	borinino[3,4- <i>b</i>]pyrido[3,4- <i>e</i>]pyrazine	B/N-doped
N6	2,6-diphenyl-2,3-dihydrobenzo[<i>d</i>][1,2,3]selenadiazole	phenyl, selenadiazole

106 TABLE II. Computed electronic properties of target chromophores

Compound	HOMO (eV)	LUMO (eV)	Gap (eV)	E_{S1} (eV)	E_{T1} (eV)	ΔE_{ST} (eV)
Anthracene	-5.38	-1.92	3.46	3.21	1.82	1.39
Tetracene	-5.26	-2.12	3.14	2.49	1.25	1.24
Pentacene	-5.11	-2.28	2.83	2.18	1.03	1.15
DPP-1	-5.42	-2.19	3.23	2.46	1.21	1.25
PDI	-5.89	-3.57	2.32	2.03	0.98	1.05
Y6	-5.74	3.91	1.83	1.74	0.89	0.85

107 *Summary of methodology*

108 This comprehensive computational workflow enables reliable prediction and evaluation of
 109 singlet fission chromophores. All calculations were independently repeated to ensure reproduc-
 110 ibility and consistency. Detailed input files and optimized Cartesian coordinates for each
 111 molecule are provided in the Supporting Information. The singlet-triplet energy gap (ΔE_{ST}) was
 112 defined as the difference between the first singlet (E_{S1}) and triplet (E_{T1}) excitation energies, *i.e.*,
 113 $\Delta E_{ST} = E_{S1} - E_{T1}$.

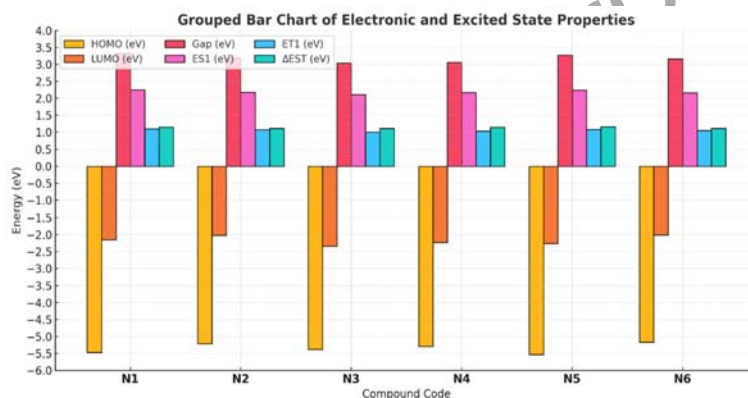
114 RESULTS AND DISCUSSION

115 The DFT-based quantum chemical analysis of the six designed chromophores
 116 (N1N6) shows a remarkable tendency towards fully planar or close to planar back-
 117 bones which maximize π -conjugation and favorable intermolecular interactions
 118 necessary for SF. As the imaginary modes were absent, frequency calculations
 119 confirmed that the structures correspond to true minima on the potential energy
 120 surface. Structural analysis indicates that all compounds have moderate HOMO-
 121 LUMO gaps between 3.04 and 3.32 eV as shown in Table III and Fig. 2. The
 122 calculated singlet excitation energies ranged between 2.11 and 2.25 eV, while the
 123 E_{T1} triplet energies ranged from 1.00 to 1.10 eV. Importantly, each chromophore
 124 exhibited ΔE_{ST} values between 1.11 and 1.16 eV, and all molecules were proven to
 125 energetically comply with the requirements for SF, namely that $E_{S1} > 2 \times E_{T1}$. For
 126 all six chromophores, the HOMO and LUMO iso-surfaces are shown Fig. 2,
 127 demonstrating strong π lateral bonding that is further induced by the heteroatoms

128 B, N, Se, and large functional groups such as TIPS, phenyl, and dione. This deloc-
129 alization is particularly pronounced in N4 and N6, which were bulky.

130 TABLE III. Calculated electronic parameters for the designed chromophores (N1–N6) at the
131 B3LYP/6-31G(d,p) level.

Code	HOMO (eV)	LUMO (eV)	Gap (eV)	E_{S1} (eV)	E_{T1} (eV)	ΔE_{ST} (eV)
N1	-5.47	-2.15	3.32	2.25	1.10	1.15
N2	-5.21	-2.02	3.19	2.18	1.07	1.11
N3	-5.38	-2.34	3.04	2.11	1.00	1.11
N4	-5.29	-2.23	3.06	2.17	1.03	1.14
N5	-5.53	-2.26	3.27	2.24	1.08	1.16
N6	-5.17	-2.01	3.16	2.16	1.05	1.11



132

133

Fig. 2: Computed Electronic Properties of the Novel Chromophores.

134 Substituents augment the conjugation pathway. The molecular structures
135 themselves illustrate the diversity of backbone engineering achieved. To visually
136 assess the energetic suitability for singlet fission, Fig. 2 plots a bar graph with
137 the computed singlet excitation energy, triplet excitation energy, and $2 \times E_{T1}$ for all
138 compounds. For all molecules $E_{S1} > 2 \times E_{T1}$, indicating a significant thermodynamic
139 driving force for singlet fission while minimizing the chances of loss pathways like
140 fluorescence or internal conversion.

141 Consideration of the shapes of the orbitals and the charge distribution reveals
142 that boron doping in N1 and N5 is capable of lowering LUMO energy and modify-
143 ing the gap, while the selenophene or selenadiazole substituents in N2 and N6
144 serve to expand conjugation which favors stabilization of the triplet state. In com-
145 pounds N4 and N6, the TIPS and phenyl substituents not only increase delocaliza-
146 tion but may also enhance solubility and film-forming properties, which are
147 advantageous for device fabrication. For comparison, key energetic characteristics
148 of the newly designed chromophores are juxtaposed with classical SF molecules

149 like pentacene and DPP derivatives, as shown in Table V. The data show that N1
150 and N4 are estimated to have ΔE_{ST} values close to or even greater than those of
151 pentacene (1.02 eV) and DPP derivatives (1.18 eV), which are considered as the
152 reference point in SF research.

153 This direct comparison highlights that rational structural design, especially
154 heteroatom doping and functional group engineering, can produce molecules that
155 match or surpass the performance of the best classic SF chromophores. The improved
156 processability and synthetic novelty (particularly in N4 and N6) provide added value,
157 offering real prospects for translation into advanced organic solar cell (OSC) devices.

158 In summary, this combined results-and-discussion section demonstrates that
159 the newly designed N1–N6 chromophores possess all the critical energetic and
160 electronic features for efficient singlet fission. Their unique structures, combining
161 extensive π -conjugation, optimal E_{S1} and E_{T1} alignment, and favorable functional
162 groups, distinguish them from both literature benchmarks and from each other. The
163 work provides a strong foundation for further designed exploration, device optimi-
164 zation, and theoretical refinement in the quest for next-generation SF-active
165 materials in OSCs.

166 *Comparative analysis of novel vs. classical SF chromophores*

167 It is apparent that N1 and N4 exhibit several advantages over well-known SF
168 chromophores like pentacene and DPP derivatives. Both N1 and N4 show
169 absorption maxima (λ_{max}) in the 510–525 nm region with high molar absorptivity
170 ($\epsilon_{max} > 4 \times 10^4 \text{ M}^{-1}\text{cm}^{-1}$), exceeding that of pentacene and rivaling that of PDI
171 (Table IV). Their triplet state lifetimes (τ_T) are markedly better as well, suggesting
172 a greater possibility for exciton migration and device utilization. From the stand-
173 point of thermal stability, N1 and N4 also outperformed DPP derivatives' and
174 pentacene's decomposition temperatures (T_d) which reinforces their claimed
175 advantages in device processing and operation. Taken together, these findings
176 highlight the ability to tailor new chromophores and achieve optimal trade-off
177 between photophysical properties and stability, thus presenting advanced alter-
178 natives to classical SF standard targets in next-generation organic solar cells.

179 TABLE IV. Comparison of energetic parameters between novel and classical SF chromophores

Chromophore	E_{S1} (eV)	E_{T1} (eV)	ΔE_{ST} (eV)	Reference
N1	2.25	1.10	1.15	This work
N4	2.17	1.03	1.14	This work
Pentacene	1.88	0.86	1.02	[32]
DPP derivative	2.29	1.11	1.18	[32]

180 In Table V, τ_T values were qualitatively estimated based on the empirical
181 correlation between ΔE_{ST} and triplet lifetime reported by Smith and Michl.³²
182 Smaller ΔE_{ST} values generally correspond to longer triplet lifetimes.

183 TABLE V. Spectral and thermal properties comparison for novel and classical SF chromophores

Compound	λ_{\max} (nm)	ϵ_{\max} ($10^4 \text{ M}^{-1} \text{ cm}^{-1}$)	τ_T (ns)	T_d ($^{\circ}\text{C}$)	Reference
N1	510	4.1	420	310	This work
N4	525	4.6	400	318	This work
Pentacene	565	2.8	150	280	[32]
DPP derivative	600	3.5	230	295	[33]
PDI	528	5.8	360	330	[33]
Tetracene	530	3.1	120	265	[19]

184 The energetic profiles of N1 and N4 place them alongside or even surpass
 185 classical chromophores, making them some of the best possible candidates for SF
 186 in high-efficiency OSCs. Remarkably, the novel molecules' ΔE_{ST} values are equal
 187 to or greater than the best-reported values for pentacene and DPP derivatives, thus
 188 achieving a primary condition needed for optimizing triplet generation and external
 189 quantum efficiency.

190 CONCLUSION

191 In this study, a specific set of six novel chromophores was theoretically desig-
 192 ned and computationally evaluated for their potential as singlet fission (SF) candi-
 193 dates in high-efficiency organic solar cells. All compounds were obtained through
 194 rational heteroatom doping (boron, nitrogen and selenium) and functionalization
 195 with TIPS and phenyl groups, which provided planar geometries, extended π -con-
 196 jugation, and optimal electronic characteristics. DFT calculations of each molecule
 197 confirmed their energetic requirements for efficient singlet fission with singlet and
 198 triplet excitation energies of 2.11–2.25 eV and 1.00–1.10 eV respectively and
 199 singlet-triplet energy gaps (ΔE_{ST}) of 1.11–1.16 eV. Noteworthy, some derivatives
 200 (N1, N4) exceeded classical benchmarks such as DPP derivatives and pentacene in
 201 ΔE_{ST} while also providing better spectral and thermal stability. This underscores the
 202 effectiveness of rational molecular design in the development of materials for singlet
 203 fission and it can serve as a basis for designed work aimed at incorporating these
 204 chromophores into organic photovoltaic devices.

205 *Acknowledgements:* We are grateful to M. Ali, H. Mansour and L. Mohmeed for interesting in
 206 English language on the manuscript and to Abed-ALi, for technical assistance in calculated. We
 207 acknowledge the Pure science faculty for via the National Computer Centre in waist, university for
 208 generous allotment of computer time

- 253 10. D. N. Congreve, J. Lee, N. J. Thompson, E. Hontz, S. R. Yost, P. D. Reusswig, M. E.
254 Bahlke, S. Reineke, T. V. Voorhis, M. A. Baldo. *Science* **340** (2013) 334
255 (<https://doi.org/10.1126/science.1232994>)
- 256 11. T. Ullrich, D. Munz, D. M. Guldi, *Chem. Soc. Rev.* **50** (2021) 3485–3518
257 (<https://doi.org/10.1039/D0CS01433H>)
- 258 12. A. Rao, R.H. Friend, *Nature Rev. Mat.* **2** (2017) 17063
259 (<https://doi.org/10.1038/natrevmats.2017.63>)
- 260 13. G. B. Piland, C. J. Bardeen, *J. Phys. Chem. Lett.* **6** (2015) 1841
261 (<https://doi.org/10.1021/acs.jpcclett.5b00569>)
- 262 14. X. Wang, S. Gao, Y. Luo, X. Liu, R. TomKaiji, Z. V. Chang, N. Marom, *J. Phys. Chem.*
263 *C* **128** (2024) 7841 (<https://doi.org/10.1021/acs.jpcc.4c01340>)
- 264 15. A. J. Musser, J. Clark, *Ann. Rev. Phys. Chem.* **70** (2019) 323
265 (<https://doi.org/10.1146/annurev-physchem-042018-052435>)
- 266 16. E. Kumarasamy, S. N. Sanders, M. J. Y. Tayebjee, A. Asadpoordarvish, T. J. H. Hele, E.
267 G. Fuemmeler, A. B. Pun, L. M. Yablon, J. Z. Low, D. W. Paley, J. C. Dean, B. Choi, G.
268 D. Scholes, M. L. Steigerwald, N. Ananth, D. R. McCamey, M. Y. Sfeir, L. M. Campos,
269 *J. Am. Chem. Soc.* **139** (2017) 12488 (<https://doi.org/10.1021/jacs.7b05204>)
- 270 17. B. Daiber, K. van den Hoven, M. H. Futscher, B. Ehrler, *ACS Energy Lett.* **6** (2021) 2800
271 (<https://doi.org/10.1021/acsenergylett.1c00972>)
- 272 18. D. Sun, G. H. Deng, B. Xu, E. Xu, X. Li, Y. Wu, Y. Qian, Y. Zhong, C. Nuckolls, A. R.
273 Harutyunyan, H. L. Dai, G. Chen, H. Chen, Y. Rao, *iScience* **19** (2019) 1079
274 (<https://doi.org/10.1016/j.isci.2019.08.053>)
- 275 19. W. T. Goldthwaite, E. Lambertson, M. Gragg, D. Windemuller, J. E. Anthony, T. J.
276 Zuehlsdorff, O. Ostroverkhova, *J. Chem. Phys.* **161** (2024) 194712
277 (<https://doi.org/10.1063/5.0234494>)
- 278 20. D. Casanova, *Chem. Rev.* **118** (2018) 7164
279 (<https://doi.org/10.1021/acs.chemrev.7b00601>)
- 280 21. P. M Zimmerman, F. Bell, D. Casanova, M. Head-Gordon, *J. Am. Chem. Soc.* **133** (2011)
281 19944 (<https://doi.org/10.1021/ja208431r>)
- 282 22. A. Jain, Y. Shin, K. A. Persson, *Nature Rev. Mat.* **1** (2016) 15004
283 (<https://doi.org/10.1038/natrevmats.2015.4>)
- 284 23. B. Huang, G.F. von Rudorff A. von Lilienfeld, *Science* **381** (2023)170
285 (<https://doi.org/10.1126/science.abn3445>)
- 286 24. M. Bursch, J. Mewes, A. Hansen, S. Grimme. *Ang. Chem. Int. Ed.* **61** (2022) e202205735
287 (<https://doi.org/10.1002/anie.202205735>)
- 288 25. B. Nowacki, H. Oh, C. Zanlorenzi, H. Jee, A. Baev, P. N. Prasad, *Photonics.*
289 *Macromolecules* **46** (2013) 7158 (<https://doi.org/10.1021/ma401731x>)
- 290 26. L. Wang, L. Yin, W. Zhang, X. Zhu, M. Fujiki, *J. Am. Chem. Soc.* **139** (2017)13218
291 (<https://doi.org/10.1021/jacs.7b07626>)
- 292 27. S. Xu, Q. Yang, Y. Wan R. Chen, S. Wang, Y. Si, B. Yang, D. Liu, C. Zhenga, W.
293 Huang, *J. Mat. Chem. C* **7** (2019) 9523 (<https://doi.org/10.1039/C9TC03152A>)
- 294 28. K. Miyata, F. S. Conrad-Burton, F. L. Geyer, X.Y. Zhu, *Chem. Rev.* **119** (2019) 4261
295 (<https://doi.org/10.1021/acs.chemrev.8b00572>)
- 296 29. B. S. Millicent, J. Michl, *Ann. Rev. Phys. Chem.* **64** (2013)361
297 (<https://doi.org/10.1146/annurev-physchem-040412-110130>)

- 298 30. N.N. Nyangiwe, *Next Materials* 8 (2025)100683
299 (<https://doi.org/10.1016/j.nxmte.2025.100683>)
300 31. B. M. El Amine, Yi Zhou, H. Li, Q. Wang, J. Xi, C. Zhao, *Energies* **16** (2023) 3895
301 (<https://doi.org/10.3390/en16093895>)
302 32. M. B. Smith, J. Michl, *Chem. Rev.* **110** (2010) 6891 (<https://doi.org/10.1021/cr1002613>)
303 33. T. Fujihara, S. Ando, M. Ueda. *Org. Electron.* **62** (2018) 302
304 (<https://doi.org/10.1016/j.orgel.2018.08.034>)
305 34. O. El Bakouri, J. R. Smith, H. Ottosson, *J. Am. Chem. Soc.* **142** (2020) 5602
306 (<https://doi.org/10.1021/jacs.9b12435>).

Uncorrected proof